

# Computation of the Real Zeros of the Kummer Function $M(a; c; x)$

Alfredo Deaño<sup>1</sup>, Amparo Gil<sup>2</sup>, and Javier Segura<sup>2</sup>

<sup>1</sup> Departamento de Matemáticas. Univ. Carlos III de Madrid. 28911, Leganés (Madrid), Spain

<sup>2</sup> Departamento de Matemáticas, Estadística y Computación. Univ. de Cantabria. 39005, Santander, Spain

**Abstract.** An algorithm for computing the real zeros of the Kummer function  $M(a; c; x)$  is presented. The computation of ratios of functions of the type  $M(a+1; c+1; x)/M(a; c; x)$ ,  $M(a+1; c; x)/M(a; c; x)$  plays a key role in the algorithm, which is based on global fixed-point iterations. We analyse the accuracy and efficiency of three continued fraction representations converging to these ratios as a function of the parameter values. The condition of the change of variables appearing in the fixed point method is also studied. Comparison with implicit Maple functions is provided, including the Laguerre polynomial case.

## 1 Introduction

Our algorithm is based on global fixed point iterations which apply to families of functions satisfying first order linear difference differential equations with continuous coefficients. The methods were described in [1,2]. The starting point of the methods is the construction of a first order system of differential equations:

$$\begin{aligned} y'(x) &= \alpha(x)y(x) + \delta(x)w(x) \\ w'(x) &= \beta(x)w(x) + \gamma(x)y(x), \end{aligned} \tag{1}$$

with continuous coefficients  $\alpha(x)$ ,  $\beta(x)$ ,  $\gamma(x)$  and  $\delta(x)$  in the interval of interest  $I$ , relating our problem function  $y(x)$  with a contrast function  $w(x)$ , whose zeros are interlaced with those of  $y(x)$ . The coefficients  $\delta(x)$  and  $\gamma(x)$  satisfy the condition  $\delta(x)\gamma(x) < 0$ , which has to be met when  $y(x)$  or  $w(x)$  have at least two zeros in the interval  $I$ .

With these restrictions, we introduce new functions and a new variable as follows. First, we consider a change of the dependent functions:

$$y(x) = \lambda_y(x)\bar{y}(x), \quad w(x) = \lambda_w(x)\bar{w}(x), \tag{2}$$

with  $\lambda_y(x) \neq 0$ ,  $\lambda_w(x) \neq 0 \forall x \in I$  in such a way that  $\bar{y}$  and  $\bar{w}$  satisfy:

$$\begin{aligned} \bar{y}' &= \bar{\alpha}\bar{y} + \bar{\delta}\bar{w} \\ \bar{w}' &= \bar{\beta}\bar{w} + \bar{\gamma}\bar{y} \end{aligned} \tag{3}$$

with  $\bar{\delta} > 0$  and  $\bar{\delta} = -\bar{\gamma}$ . This is accomplished by choosing:

$$\lambda_y = \text{sign}(\delta)\lambda_w\sqrt{-\delta/\gamma} \quad (4)$$

It is obvious that the new functions  $\bar{y}(x)$  and  $\bar{w}(x)$  have the same zeros as  $y(x)$  and  $w(x)$ . Considering now a change of variables:

$$z(x) = \int \bar{\delta}(x)dx, \quad (5)$$

the system reads:

$$\begin{pmatrix} \dot{\bar{y}} \\ \dot{\bar{w}} \end{pmatrix} = \begin{pmatrix} \bar{a} & 1 \\ -1 & \bar{b} \end{pmatrix} \begin{pmatrix} \bar{y} \\ \bar{w} \end{pmatrix}, \quad (6)$$

where  $\bar{a} = \bar{\alpha}/\bar{\delta}$ ,  $\bar{b} = \bar{\beta}/\bar{\delta}$  and dots mean derivative with respect to  $z$ . Then, the ratio  $H(z) = \bar{y}/\bar{w}$  satisfies the first order non-linear ODE:

$$\dot{H} = 1 + H^2 - 2\eta H, \quad (7)$$

where  $\eta = (\bar{b} - \bar{a})/2$ .

From Eq.(7) it is possible to build a fixed point iteration [1]:

$$T(z) = z - \arctan(H(z)), \quad (8)$$

which converges globally to the zeros of  $H(z)$  in intervals where the function  $\eta$  does not change sign [1]. These zeros are the same as those of the function  $\bar{y}(z)$ , and undoing the change of variable we obtain the zeros of  $y(x)$  in the original variable  $x$ .

## 2 The Confluent Hypergeometric Function $M(a; c; x)$

We consider the Kummer differential equation:

$$xy''(x) + (c - x)y'(x) - ay(x) = 0. \quad (9)$$

This equation has a regular singular point at the origin and an irregular singularity at infinity. The regular solution around the origin reads

$$M(a; c; x) = \sum_{n=0}^{\infty} \frac{(a)_n}{(c)_n} \frac{x^n}{n!}, \quad (10)$$

where  $(a)_n = a(a+1)(a+2)\dots(a+n-1)$  is the usual Pochhammer symbol. This power series has radius of convergence equal to infinity, and defines for all complex values of  $a, c, x$  (except if  $c = 0, -1, -2, \dots$ ) a function which is a hypergeometric function of type  ${}_1F_1$  and it is known as *confluent hypergeometric function of the first kind* or *Kummer function*.

In this paper we will focus on real values of  $a$ ,  $c$  and  $x$ . Moreover, we can restrict ourselves to  $x > 0$ , because by Kummer transformations [3]:

$$M(a; c; x) = e^x M(c - a; c; -x). \quad (11)$$

The positive real zeros of the function  $M(a; c; x)$  are bounded, a property that can be proved by writing (9) in normal form. Indeed, the functions  $w(x) = x^{c/2} e^{-x/2} y(x)$  with  $y(x)$  solution of (9), satisfy

$$w''(x) + \left( -\frac{1}{4} + \frac{c-2a}{2x} + \frac{c(2-c)}{4x^2} \right) w(x) = 0. \quad (12)$$

It is straightforward to check that the turning points are:

$$x_{\pm} = c - 2a \pm \sqrt{(c-2a)^2 + c(2-c)}. \quad (13)$$

When  $x > x_+$  and when  $x < x_-$  the independent term in (12) is negative, and as a consequence of Sturm theorems [10] the function  $M(a; c; x)$  can only have at most one zero in that region. More precisely, in [4] it is shown that if  $M(a; c; x)$  has at least two positive real zeros then the parameters verify the so called *oscillatory conditions*:

$$a < 0, \quad c - a > 1 \quad (14)$$

It is worth noticing that if  $a = -n$  is a negative integer we obtain the classical Laguerre polynomials  $L_n^{(\alpha)}(x)$ , where  $c = \alpha + 1$ .

## 2.1 Systems of DDEs for $M(a; c; x)$

Let us illustrate the construction of a system of DDEs for the functions  $M(a; c; x)$ . These functions satisfy the following relation (Eq. 13.4.11 of [3]):

$$xM'(a; c; x) = (a + x - c)M(a; c; x) + (c - a)M(a - 1; c; x) \quad (15)$$

and the following three-term recurrence relation (TTRR) (Eq.13.4.1 of [3]):

$$aM(a + 1; c; x) = (2a - c + x)M(a; c; x) + (c - a)M(a - 1; c; x) \quad (16)$$

Now, using the notation  $y_n \equiv M(a + n; c; x)$ , we can write the following system of difference-differential equations (1), as stated in [7]:

$$\begin{aligned} y'_n &= \frac{a + n + x - c}{x} y_n + \frac{c - a - n}{x} y_{n-1} \\ y'_{n-1} &= -\frac{a + n - 1}{x} y_{n-1} + \frac{a + n - 1}{x} y_n, \end{aligned} \quad (17)$$

where the second DDE can be obtained from the first DDE (15) by replacing  $n \rightarrow n - 1$  and using the TTRR (16) for expressing  $y_{n-2}$  in terms of  $y_n$  and  $y_{n-1}$ .

In this example the dependence on  $n$  is located in the first parameter of the hypergeometric function, but it is clear that other choices are available. By denoting  $a_n \equiv a + k n$ ,  $c_n \equiv c + m n$  and  $y_n \equiv M(a_n; c_n; x)$  we will have different sets of DDEs for different selections of  $(k, m)$ . As explained in the introduction, these DDEs are the starting point for building the fixed point iterations.

### 3 Ratios of Hypergeometric Functions and Continued Fractions

In order to apply the fixed point method for the real zeros of the function  $M(a; c; x)$  we will need to compute the following ratios:

$$R_{1,1}(x) := \frac{M(a+1; c+1; x)}{M(a; c; x)}, \quad (18)$$

when  $x < c - a$ , and

$$R_{1,0}(x) := \frac{M(a+1; c; x)}{M(a; c; x)}, \quad (19)$$

when  $x > c - a$ . The selection of the  $x$ -range is based on the efficiency of the associated fixed point methods, as explained in [7].

As it is well known, confluent hypergeometric functions satisfy three-term recurrence relations in any direction of increasing (decreasing) parameters (with integer values), and the associated continued fractions converge to the ratio of minimal solutions of the recurrence by Pincherle's theorem [8,10] and when the recurrence has a minimal solution. However, great care is needed in order to avoid situations of pseudoconvergence of the continued fractions, as explained in [5], that may result in a loss of precision in the computation or even in the computation of a wrong ratio of functions.

When  $x < c - a$  we have to use the iteration  $(1, 1)$  (increasing both parameters), and the function  $M(a; c; x)$  is minimal in that direction. No pseudoconvergence is expected, since this phenomenon is present when  $x$  is larger than  $c$ , as can be seen in [5]. Therefore we can use the continued fraction that stems from the recursion:

$$H^{(1)}(x) := \frac{c}{c-x+} \frac{(a+1)x}{c+1-x+} \frac{(a+2)x}{c+2-x+} \cdots, \quad (20)$$

This continued fraction converges to the ratio  $R_{1,1}$  for  $x \in \mathbb{R}$ . We note that if the parameter  $a$  is a negative integer then the confluent hypergeometric function reduces to a polynomial of Laguerre type, and therefore the continued fraction is finite.

When  $x > c - a$  we have to use the ratio corresponding to the  $(1, 0)$  iteration. In this case the CF from the  $(1, 0)$  recursion can not be used for computing zeros of  $M(a; c; x)$ , because the function  $M(a+n; c; x)$  is dominant when  $n \rightarrow \infty$ . However, we can use the QD algorithm [8] to construct the following C-fraction from the power series expansion of (19):

$$H^{(2)}(x) := a_0 + \frac{a_1 x}{1+} \frac{a_2 x}{1+} \frac{a_3 x}{1+} \cdots, \quad (21)$$

where  $a_0 = 1$ ,  $a_1 = 1/c$ , and:

$$a_{2m} = \frac{a+1-c-m}{(c+2m-2)(c+2m-1)}, \quad m \geq 1 \quad (22)$$

$$a_{2m+1} = \frac{a+m}{(c+2m-1)(c+2m)}, \quad m \geq 1 \quad (23)$$

This CF converges to the ratio  $M(a+1; c; x)/M(a; c; x)$  on compact subsets of  $\mathbb{R}$  except for the zeros of  $M(a; c; x)$ . We refer the reader to [8, pg. 313] for a similar result for the ratio in the  $(1, 1)$  direction. However, it is important to note that this continued fraction exhibits pseudoconvergence [5] for large  $x$ , and therefore should not be used to compute the largest zeros. For moderate values of  $x$ , on the other hand, is a useful expression, as we show in Section 4.

When the variable  $x$  is large it is possible to use the fact that the function  $M(a; c; x)$  is minimal in the  $(0, 1)$  direction, that is, when we increase the parameter  $c$ . This leads to the following continued fraction:

$$\frac{c}{c+x+} \frac{-(c+1-a)x}{c+1+x+} \frac{-(c+2-a)x}{c+2+x+} \dots, \quad (24)$$

This continued fraction converges to the ratio  $M(a; c+1; x)/M(a; c; x)$ , and it does not present pseudoconvergence if the oscillatory conditions are fulfilled. Once computed, we can obtain the ratio in the  $(1, 0)$  direction by means of a three-term recurrence relation [3]:

$$\frac{M(a+1; c; x)}{M(a; c; x)} = \frac{c}{c-x} \frac{M(a+1; c+1; x)}{M(a+1; c; x)} \quad (25)$$

This gives the following continued fraction for the ratio  $R_{1,0}(x)$ :

$$H^{(3)}(x) := \frac{1}{1+} \frac{-x}{c+x+} \frac{-(c-a)x}{c+1+x+} \frac{-(c+1-a)x}{c+2+x+} \frac{-(c+2-a)x}{c+3+x+} \dots, \quad (26)$$

## 4 Computational Aspects of Continued Fractions

The algorithm uses the modified Lentz-Thompson method [9] to compute the continued fractions (20), (21) and (26). The first one is used when  $x < c - a$ , and the other two when  $x > c - a$ .

First, we perform an analysis of the accuracy of the continued fractions used in the algorithm, comparing with the internal Maple subroutine `KummerM(a, c, x)`. In the following plots we have fixed several values of the parameter  $a$  and we have used a random sweep in the plane  $(c, x)$ . The threshold of accuracy has been set to five digits less than the working precision (40 digits). Dark dots denote points where the relative error between the continued fraction used and Maple is smaller than this quantity, and grey dots when it is larger. We have also plotted the line  $x = c - a$  in the case of the first continued fraction, and both  $x = c - a$  and  $x = c - 2a$  in the other two cases.

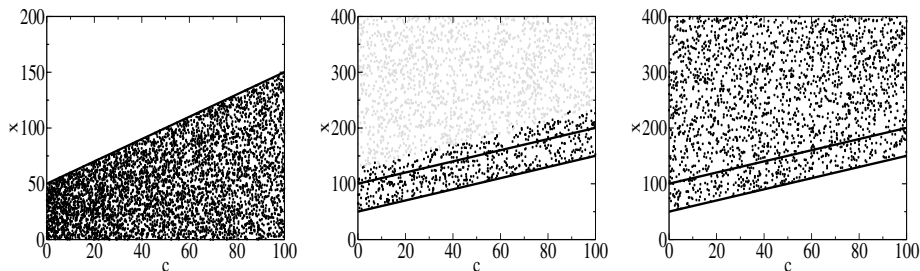


**Fig. 1.** Plots for  $a = -50.1$ , with a sweep of 5000 random points. Left: accuracy test for the CF (20) when  $x < c - a$ . Center: accuracy test for the CF (21) when  $x > c - a$ . We observe a loss of accuracy of the CF when  $x$  becomes large. Right: accuracy test for the CF (24) when  $x > c - a$ . We include the lines  $x = c - a$  (left) and both  $x = c - a$  and  $x = c - 2a$  (center and right).

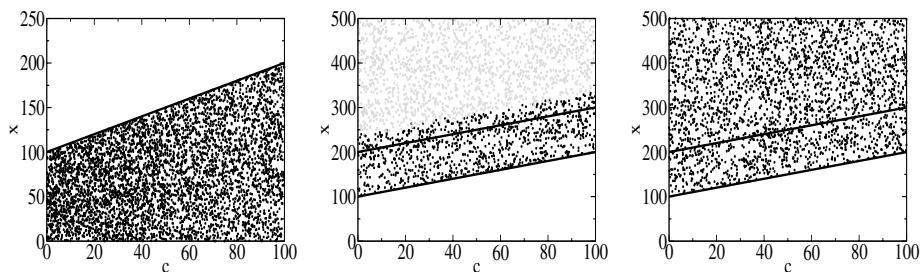


**Fig. 2.** Plots for  $a = -100.1$ , with a sweep of 5000 random points. Left: accuracy test for the (20) when  $x < c - a$ . Center: accuracy test for the CF (21) when  $x > c - a$ . We observe a loss of accuracy of the CF when  $x$  becomes large. Right: accuracy test for the CF (24) when  $x > c - a$ . We include the lines  $x = c - a$  (left) and both  $x = c - a$  and  $x = c - 2a$  (center and right).

The graphics suggest that the first continued fraction (20) can be used when  $x < c - a$ . When  $x > c - a$  and  $x$  is not too large the second one is correct, but the attainable accuracy deteriorates when  $x$  becomes large. This loss of accuracy corresponds to the continued fraction (21), because the third continued fraction (24) agrees with Maple subroutine in the whole region, as can be seen in the graphics on the right.

In the general algorithm we will change from (21) to (24) when  $x = c - 2a$ . This choice seems to be safe according to numerical experiments, and it can be justified by performing a canonical contraction of (21), as explained in [8, pg.83]. In the resulting continued fraction both the numerators and the denominators change of sign (from negative to positive), taking into account (14). When  $x < c - 2a + 1$  the change in the denominator occurs when the numerators are still negative, and therefore there is no risk of pseudoconvergence (see [5] for the criterion

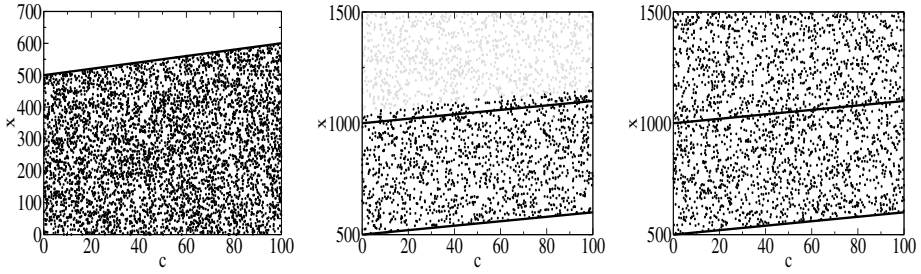


**Fig. 3.** Plots for  $a = -500.1$ , with a sweep of 5000 random points. Left: accuracy test for the CF (20) when  $x < c - a$ . Center: accuracy test of the CF (21) when  $x > c - a$ . We observe a loss of accuracy of the CF when  $x$  becomes large. Right: accuracy test for the CF (24) when  $x > c - a$ . We include the lines  $x = c - a$  (left) and  $x = c - 2a$  (center and right).

of signs). On the other hand, when  $x > c - 2a + 1$  the denominator changes from negative to positive when the numerators are already positive. This is a distinctive sign of pseudoconvergence and causes the loss of accuracy observed in the plots.

#### 4.1 Timings

From the point of view of accuracy, numerical tests indicate that it is possible to use the third continued fraction (24) when  $x > c - a$ . However, the continued fraction (21) seems to be more efficient for moderate values of  $x$  in terms of CPU time, so we have kept the three continued fractions in the program to test CPU time. If we compare both continued fractions in the zone  $c - a < x < c - 2a$  we obtain that (21) is generally faster, as shown in Figure 4.

Once accuracy is tested we have to compare CPU times for continued fraction evaluation and Maple, in order to establish which is the most efficient method depending on the parameters.

Timing tests have been performed again fixing different values of  $a$ , carrying out random sweeps in  $c$  and  $x$  and comparing the result from the continued fraction method with the intrinsic Maple procedure (Figure 5). In order to ensure a significant number of calls to both algorithms repeating loops are included, which use slightly different values of the parameters in each call, in such a way that the values are actually recomputed, and not stored in memory. Black dots represent points where the continued fraction is faster, whereas grey dots indicate that Maple is more efficient.

After several tests for fixed values of  $a$  the continued fraction method seems to be superior when  $x$  and/or  $a$  are large, whereas Maple is faster for large values of  $c$ . A final least squares fit is calculated to obtain a condition in terms of the parameters of the function that will enable us to choose the best method in the general algorithm.

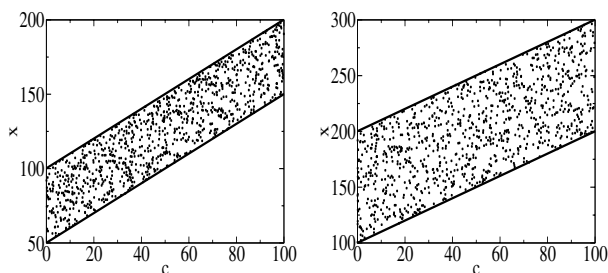


**Fig. 4.** Timings of continued fractions (21) and (24) in the region  $c - a < x < c - 2a$ . We include both lines. Left,  $a = -50.1$ . Right:  $a = -100.1$ . 1000 random points have been used in the region  $c - a < x < c - 2a$ , and points indicate where (21) is faster.

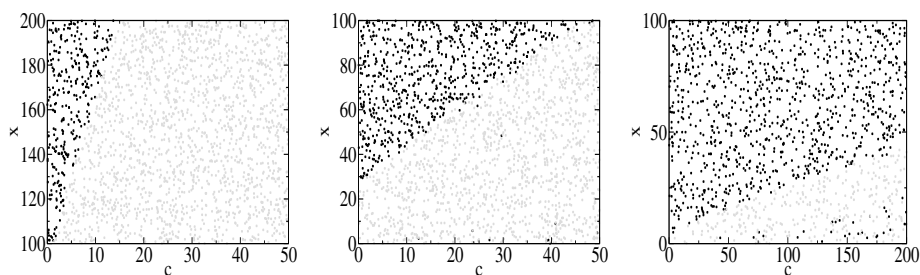


**Fig. 5.** Comparison between continued fractions (20), (21), (24) and Maple in the final scheme. Left:  $a = -50.1$ . Center:  $a = -100.1$ . Right:  $a = -500.1$ . 2000 random points have been used in each case. Black points indicate where continued fraction is faster, grey points where Maple is more efficient.

Apart from the numerical results shown before in the plots, similar graphics have been generated in the cases  $a = -75.1, -125.1, -150.1, -200.1, -250.1, -300.1, -325.1, -350.1, -400.1, -425.1, -450.1$ , using random sweeps in the plane  $(c, x)$ , in order to obtain a finer fit.

For each value of  $a$ , a straight line in the plane  $(c, x)$  divides approximately the zones where Maple or the continued fraction are superior. These lines have the form  $x = mc + l$ , where  $m, l$  are positive and decreasing when  $|a|$  increases (see Figure 5). We have used a least squares fit to adjust the values of  $m$  and  $l$ , for values of  $|a|$  between 50 and 500, and we have obtained the following function:

$$f(a, c, x) = -x + \frac{A_1}{(-a)^{A_2}}c + \frac{A_3}{(-a)^{A_4}}, \quad (27)$$

where the constants  $A_1, A_2, A_3$  and  $A_4$  are:

$$A_1 = 2408.3405, A_2 = 1.5448166, A_3 = 5182.0407, A_4 = 1.0234031.$$

Given  $a, c$  and  $x$ , the continued fraction method should be used if  $f(a, c, x) < 0$ . Several tests have been carried out to check if this fit is correct: we have



computed random values of  $a$ ,  $c$  and  $x$  in the intervals  $(-500, -50)$ ,  $(0, 200)$  and  $(0, 1000)$  respectively, and we have checked again the timings of the continued fraction method and Maple whenever  $f(a, c, x) < 0$ . If the fit is correct, this test should be favourable to the continued fraction method. In all cases, the proportion of points in the regions considered where the continued fraction is actually faster than Maple is larger than 90%.

## 5 Building the Full Algorithm

The main ingredients of the algorithm for computing the real zeros of hypergeometric functions were discussed in [7]. The resulting algorithm for computing the real zeros of the Kummer function  $M(a; c; x)$ , in a given interval  $I = (x_a, x_b)$  reads as follows:

◦ Consider the following functions:

$$\begin{aligned} z_1(x) &= 2\sqrt{(1-a)x}, \\ H_1(x) &= \sqrt{\left| \frac{(1-a)x}{(c-1)^2} \right|} \frac{M(a; c; x)}{M(a-1; c-1; x)}, \\ \eta_1(x) &= -\frac{2x+3-2c}{4\sqrt{(1-a)x}}, \end{aligned}$$

and

$$\begin{aligned} z_2(x) &= \sqrt{(c-a)(1-a)} \log x, \\ H_2(x) &= \sqrt{\left| \frac{1-a}{c-a} \right|} \frac{M(a; c; x)}{M(a-1; c; x)}, \\ \eta_2(x) &= -\frac{2a+c+x}{2\sqrt{(c-a)(1-a)}}. \end{aligned}$$

◦ Let  $x_{tran} = c - a$ .

If  $x_b < x_{tran}$ , consider  $z(x) = z_1(x)$ ,  $H(x) = H_1(x)$ ,  $\eta(x) = \eta_1(x)$ .

If  $x_b > x_{tran}$ , let  $I_1 = (x_a, x_{tran})$ ,  $I_2 = (x_{tran}, x_b)$ . Then consider

$$z(x) = z_1(x), H(x) = H_1(x), \eta(x) = \eta_1(x) \text{ in } I_1 \text{ and } z(x) = z_2(x), H(x) = H_2(x), \eta(x) = \eta_2(x) \text{ in } I_2.$$

◦ Divide the interval  $I$  (or the corresponding subintervals  $I_1, I_2$ ) in subintervals where  $\eta(x)$  does not change sign.

◦ Apply the following routine (*SWEEP*) in those subintervals where  $\eta(x)$  does not change sign, but replacing the variable  $x$  by  $z(x)$  and  $H(x)$  by  $H(z) = H(x(z))$ . The zeros are computed in the  $z$  variable. Let  $[z_1, z_2]$  be an interval where  $\eta$  does not change sign:

*SUBROUTINE SWEEP( $j, z_1, z_2, \epsilon, i, z(i)$ )*

**Algorithm: forward and backward sweeps.**

**Input:**  $j = -\text{sign}(\eta)$  (+1 forward sweep; -1 backward);  $z_1; z_2; \epsilon \equiv$  relative precision

**Output:**  $i$  (number of zeros);  $z(1), \dots, z(i)$ : zeros in the interval

$\text{NOTERM}=1$

$$\bar{z}_1 = \frac{z_1 + z_2}{2} + j\left(\frac{z_1 - z_2}{2}\right)$$

$$z = \bar{z}_1$$

$$\bar{z}_2 = \frac{z_1 + z_2}{2} - j\left(\frac{z_1 - z_2}{2}\right)$$

IF ( $jH(z) > 0$ ) THEN  $z = z + j\pi/2$

$i = 0$

DO WHILE ( $j(z - \bar{z}_2) < 0$ )

CALL FIXEDPOINT( $z, \bar{z}_2, \epsilon, z_n, \text{NOTERM}$ )

IF ( $\text{NOTERM}=1$ ) THEN

$$z(j\ i) = z_n$$

$$i = i + 1$$

$$z = z_n + j\pi/2$$

ELSE

$$z = \bar{z}_2 + j$$

ENDIF

END WHILE

END

*SUBROUTINE FIXEDPOINT( $z, \bar{z}_2, \epsilon, z_n, \text{NOTERM}$ )*

$\text{Err}=1 + \epsilon$

DO WHILE ( $\text{NOTERM}=1$ ) AND ( $\text{Err} > \epsilon$ )

$$z_p = z$$

$$z = z - \arctan(H(z))$$

$$\text{Err} = |1 - z/z_p|$$

IF ( $j(z - \bar{z}_2) > 0$ ) THEN  $\text{NOTERM}=0$

END WHILE

$$z_n = z$$

END

and the zeros generated in a forward sweep are stored in the positive positions of the array  $z(i)$  ( $z(1), z(2), \dots$ ) while those generated in a backward sweep are stored in the negative positions ( $z(-1), z(-2), \dots$ ).

- Invert the change of variable  $z(x)$  to obtain the zeros in the original variable.

A relevant issue for the stability of the full algorithm, which was not analysed in previous references [1,2,4], is the condition of the change of variables associated to the recurrences used in the algorithm. We discuss this point briefly in the following section.

## 5.1 Condition of the Change of Variables

An important issue in the accuracy of the computed zeros is the condition of the change of variable  $z = z(x)$  explained in section 1. Indeed, once the zeros are

computed in the variable  $z$  by means of the fixed point iteration, it is necessary to undo the change of variable in order to obtain the zeros in the original variable  $x$  and evaluate  $x = x(z)$  at those points. In this section we examine the two changes used for Kummer function.

As explained in [7], the changes of variable associated with the iterations  $(1, 1)$  and  $(1, 0)$  are, respectively:

$$z_1(x) = 2\sqrt{(1-a)x}, \quad z_2(x) = \sqrt{(c-a)(1-a)}\log(x). \quad (28)$$

The second change maps the interval  $(0, +\infty)$  onto  $(-\infty, +\infty)$ , and the first one onto itself. When transforming from  $z$  to  $x$  the relative condition number is:

$$\kappa_{rel} = \left| z \frac{\dot{x}(z)}{x(z)} \right|. \quad (29)$$

In the first case:

$$\kappa_{rel} = 2, \quad (30)$$

so the problem is well conditioned. In the second case:

$$\kappa_{rel} = \left| \frac{z}{\sqrt{(c-a)(1-a)}} \right|. \quad (31)$$

Hence the condition number grows linearly with the variable  $z$ . In terms of the variable  $x$  we have that  $\kappa_{rel} = |\log(x)|$ . Taking into account (Eq.13), when the parameter  $-a$  is large the largest zero is  $x \sim -4a$ , and we can estimate  $\kappa_{rel} \sim \log(-4a)$ .

For instance, for Laguerre polynomials  $L_n^{(\alpha)}(x)$  the condition number can be estimated as  $\kappa_{rel} \sim \log(4n)$  when the degree of the polynomial is large, and the loss of significant digits is mild for the large zeros. Because the corresponding fixed point iteration is only used for  $x > c - a = n + \alpha + 1 > 1$ , there is no bad condition due to  $x$  close to zero and  $\kappa_{rel} \sim \log(4n)$  in the worst case.

## 5.2 Timings

The algorithm has been coded in Maple. In Table 1 we show examples of typical CPU-times spent by the algorithm on a standard configuration PC (Intel Pentium M processor at 1.5GHz and RAM memory of 512MB) under Windows XP. We consider non polynomial and polynomial cases. In the polynomial case, we show the relative CPU-times in comparison with the computation of the zeros using the Maple functions **KummerM** and **fsolve**. The interval for computing the zeros has been fixed to  $I = [0.001, 50]$ .

**Table 1.** Typical CPU-times spent by the algorithm for computing the real zeros of the Kummer function  $M(a; c; x)$ . (\*) The number of digits for the computation with the function **fsolve** has been set to 35 in order to obtain at least 14 digits correct for the largest zero. (\*\*) The number of digits for the computation with the function **fsolve** has been set to 50 in order to obtain at least 14 digits correct for the largest zero.

$a$	$c$	$N_{zeros}$	CPU-time	RelCPU
-50.1	0.1	31	1.6 s	
-100.1	0.1	44	2.3 s	
-500.1	0.1	99	8.6 s	
-50	0.1	31	1.3 s	13.6(*)
-100	0.1	44	2.2 s	55.7(**)

## Acknowledgments

The authors thank the referee for comments which have helped in improving the final manuscript. A. Gil acknowledges financial support from *Ministerio de Educación y Ciencia (programa Ramón y Cajal)*. J. Segura acknowledges financial support from project BFM2003-06335-C03-02. The authors acknowledge financial support from *Ministerio de Educación y Ciencia* (Project MTM2004-01367).

## References

1. J. SEGURA. *The zeros of special functions from a fixed point method.*, SIAM J. Numer. Anal. 40 (2002) 114-133.
2. A. GIL AND J. SEGURA. *Computing zeros and turning points of linear homogeneous second order ODEs*, SIAM J. Numer. Anal. 41 (2003) 827-855.
3. M. ABRAMOWITZ, I. A. STEGUN. *Handbook of Mathematical functions, with formulas, graphs and mathematical tables*. Dover, 1972.
4. A. DEAÑO, A. GIL, J. SEGURA. *New inequalities from classical Sturm theorems*. J. Approx. Theory 131 (2004), 208-230.
5. A. DEAÑO, J. SEGURA. *Transitory minimal solutions of hypergeometric recursions and pseudoconvergence of associated continued fractions*. Accepted for publication in Math. Comp.
6. E. FRANK. *A new class of continued fraction expansions for the ratios of hypergeometric functions*. Transactions of the American Mathematical Society, Vol. 81, n. 2, (1956) 453-476.
7. A. GIL, W. KOEPF, J. SEGURA. *Computing the real zeros of hypergeometric functions*. Numer. Algorithms 36 (2004) 113-134.
8. L. LORENTZEN, H. WAADELAND. *Continued fractions with applications*. North Holland, 1992.
9. I.J. THOMPSON, A. R. BARNETT. *Coulomb and Bessel functions of complex arguments and order*. J. Comput. Phys. 64 (1986) 490-509.
10. N.M. TEMME. *Special functions. An introduction to the classical functions of Mathematical Physics*. John Wiley and Sons. 1996.